Supporting Information

Validating TDP1 as an inhibition target for the development of chemosensitizers for camptothecin-based chemotherapy drugs

Euphemia Leung, Jinal Patel, Jennifer Hollywood, Ayesha Zafar, Petr Tomek, David Barker, Lisa I. Pilkington, Michelle van Rensburg, Ries J. Langley, Nuala A. Helsby, Christopher J. Squire, Bruce C. Baguley, William A. Denny, Jóhannes Reynisson, Ivanhoe K. H. Leung

Supplementary Figures

(a)

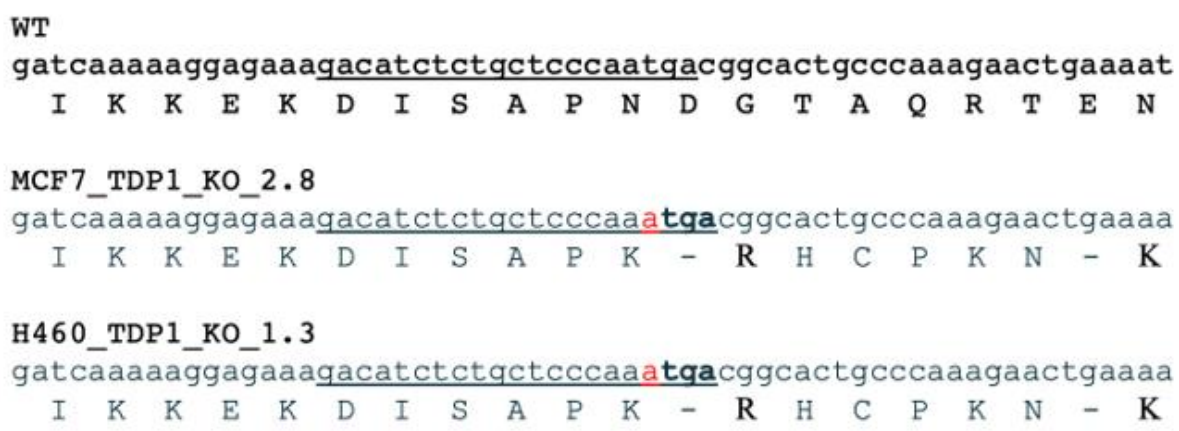

(b)

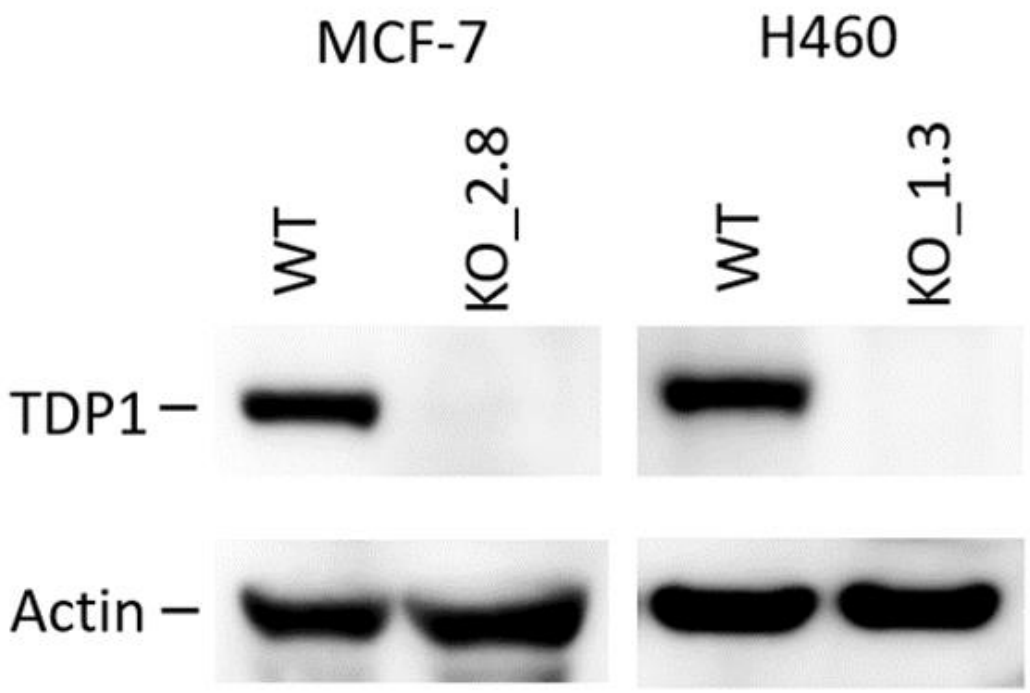

Figure S1: (a) DNA sequence analysis of TDP1-KO clones MCF7_TDP1_KO_2.8 and H460_TDP1_KO_1.3 reveal single nucleotide insertions (red) at the 3' end of the guide RNA target sequences (underlined). The frame shift caused by these insertions resulted in a stop codon in place of codon 122 in the TDP1-KO cell lines; (b) The immunoblotting of TDP1 from

MCF7 and H460 cancer cell lines. The knockout (KO) clones do not express any TDP1 as compared to their wild type (WT) counterparts, i.e., a complete ablation was reached.

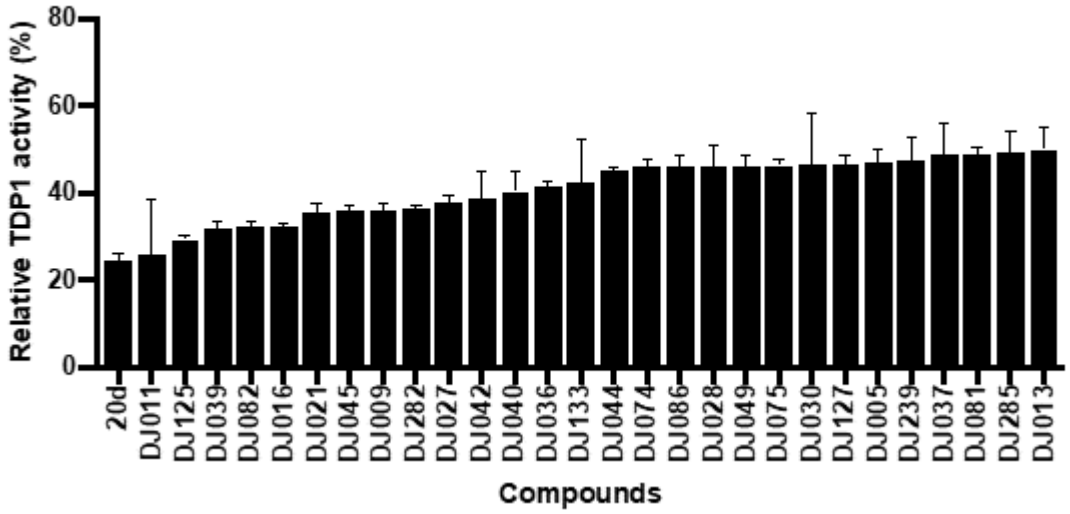

Figure S2: Bar graph of TDP1 activity using the fluorophore quencher-coupled DNA-biosensor. 128 compounds were screened at 25 µM concentration with the 28 most active compounds shown (at least 50% inhibition after 10 min). A previously reported TDP1 inhibitor (compound 20d)[1] was used as a positive control. Data are mean ± SE of n=4 replicate values.

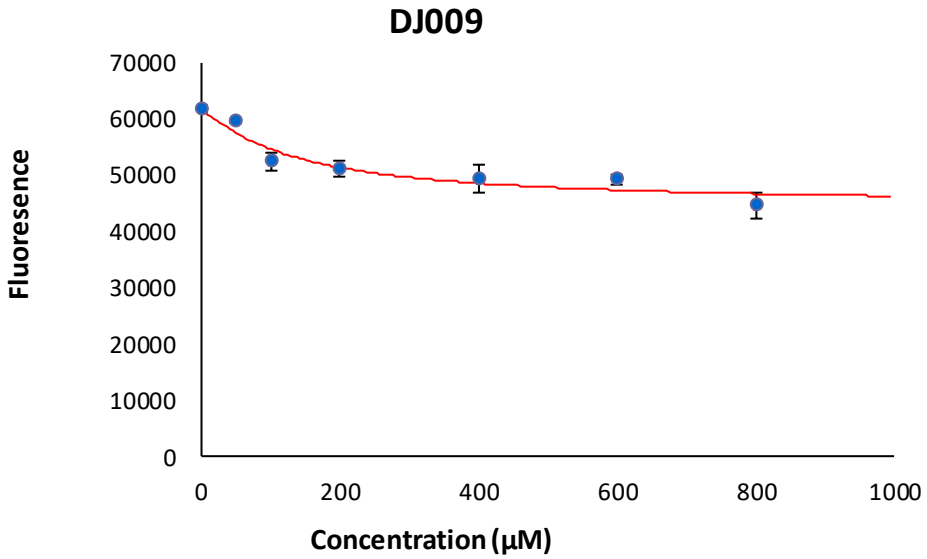

Figure S3: Changes in intrinsic fluorescence intensity of TDP1 (10 µM) upon the addition of compound DJ009. Buffer was 20 mM Tris and 250 mM NaCl (pH 8). Excitation wavelength was 280 nm and intrinsic fluorescence was measured between 300 and 450 nm. The K_D was 146 ± 111 µM. Data are mean ± SD of three independent experiments.

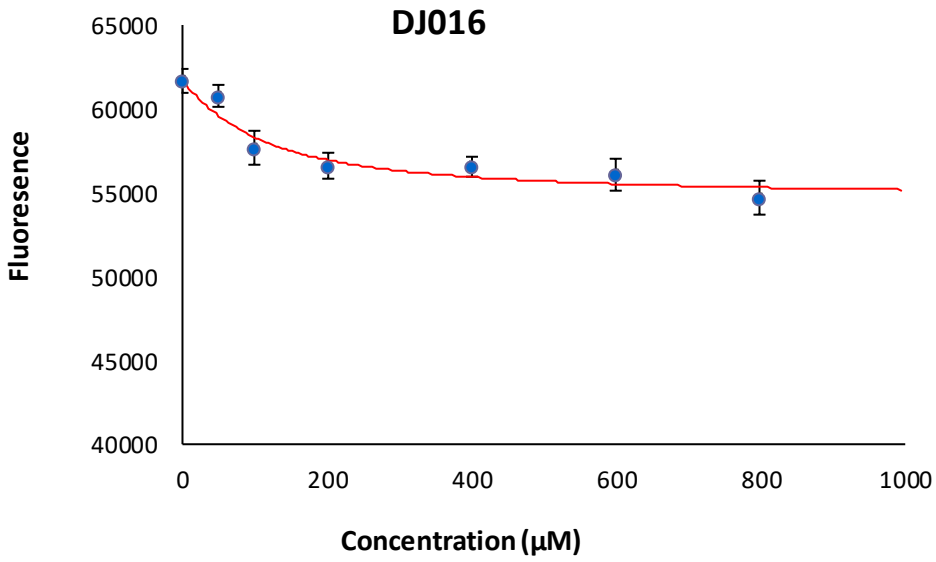

Figure S4: Changes in intrinsic fluorescence intensity of TDP1 (10 µM) upon the addition of compound DJ016. Buffer was 20 mM Tris and 250 mM NaCl (pH 8). Excitation wavelength was 280 nm and intrinsic fluorescence was measured between 300 and 450 nm. The K_D was 281 ± 28 µM. Data are mean ± SD of three independent experiments.

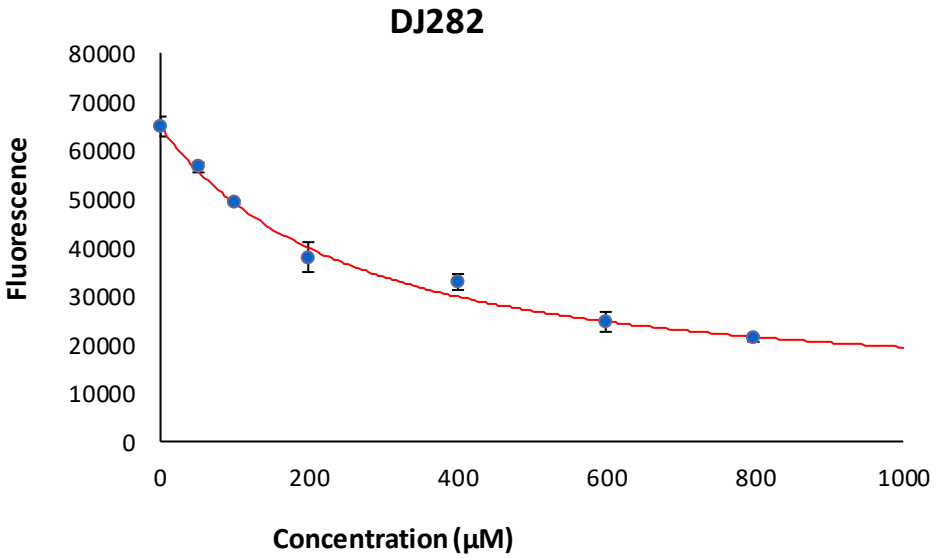

Figure S5: Changes in intrinsic fluorescence intensity of TDP1 (10 µM) upon the addition of compound DJ282. Buffer was 20 mM Tris and 250 mM NaCl (pH 8). Excitation wavelength was 280 nm and intrinsic fluorescence was measured between 300 and 450 nm. The K_D was 234 ± 64 µM. Data are mean ± SD of three independent experiments.

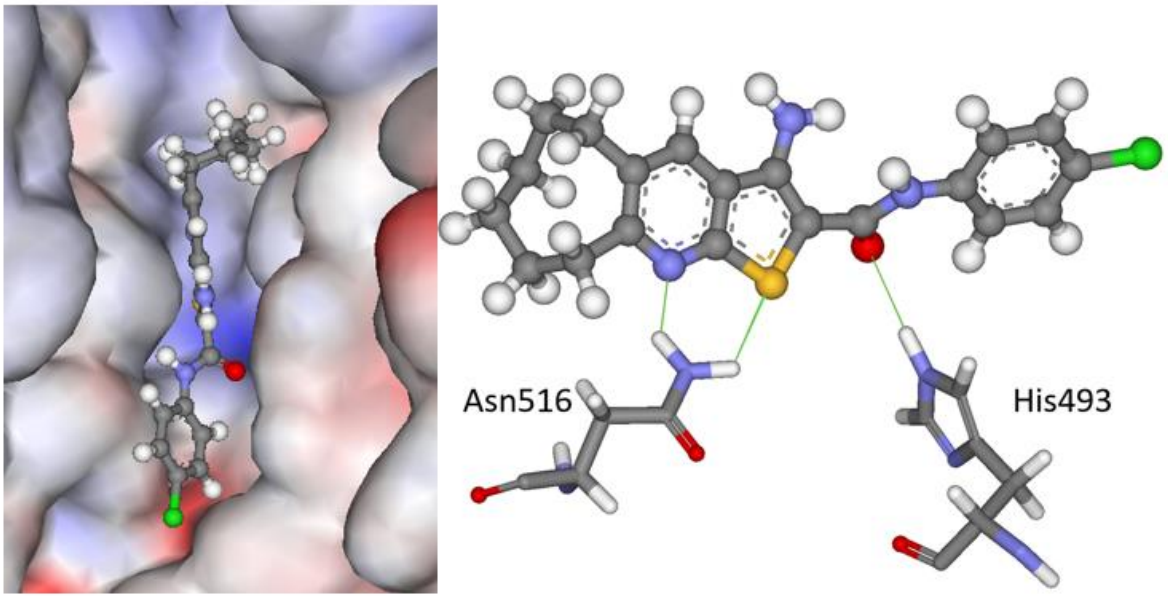

Figure S6: The docked configuration of DJ009 in the binding site of TDP1 as predicted using the GoldScore scoring function. (A) The protein surface is rendered. The ligand occupies the binding pocket blocking access to it. Blue depicts a hydrophilic region with a partial positive charge on the surface; red depicts regions with a partial negative charge and grey shows neutral areas. (B) H-bonds are shown as green lines between DJ009 and the amino acids His493 and Asn516 side groups.

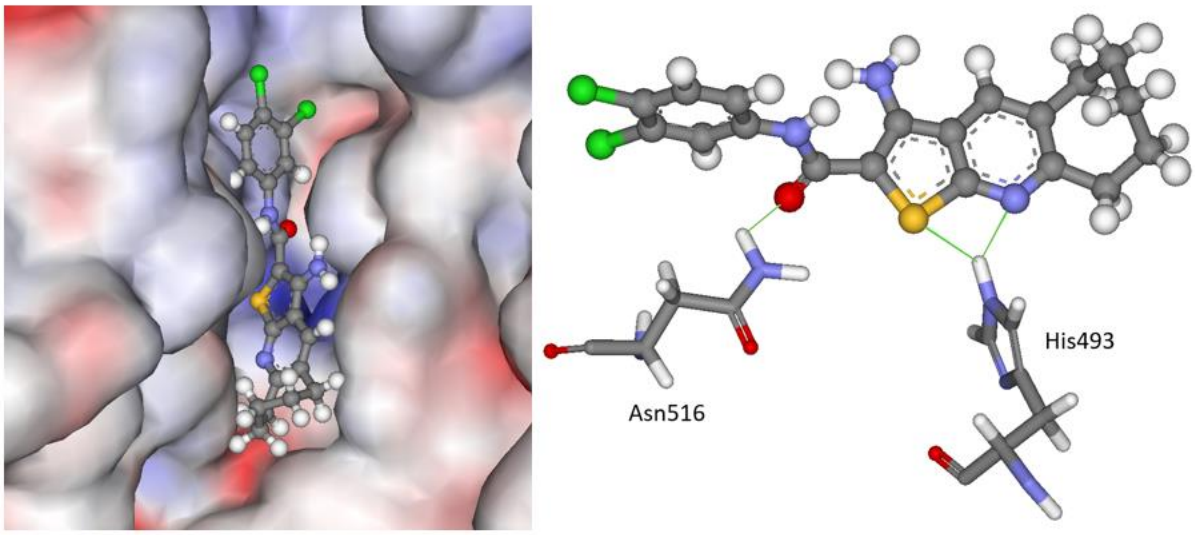

A **B**

Figure S7: The docked configuration of DJ016 in the binding site of TDP1 as predicted using the GoldScore scoring function. (A) The protein surface is rendered. The ligand occupies the binding pocket blocking access to it. Blue depicts a hydrophilic region with a partial positive charge on the surface; red depicts regions with a partial negative charge and grey shows neutral areas. (B) H-bonds are shown as green lines between DJ016 and the amino acids His493 and Asn516 side groups.

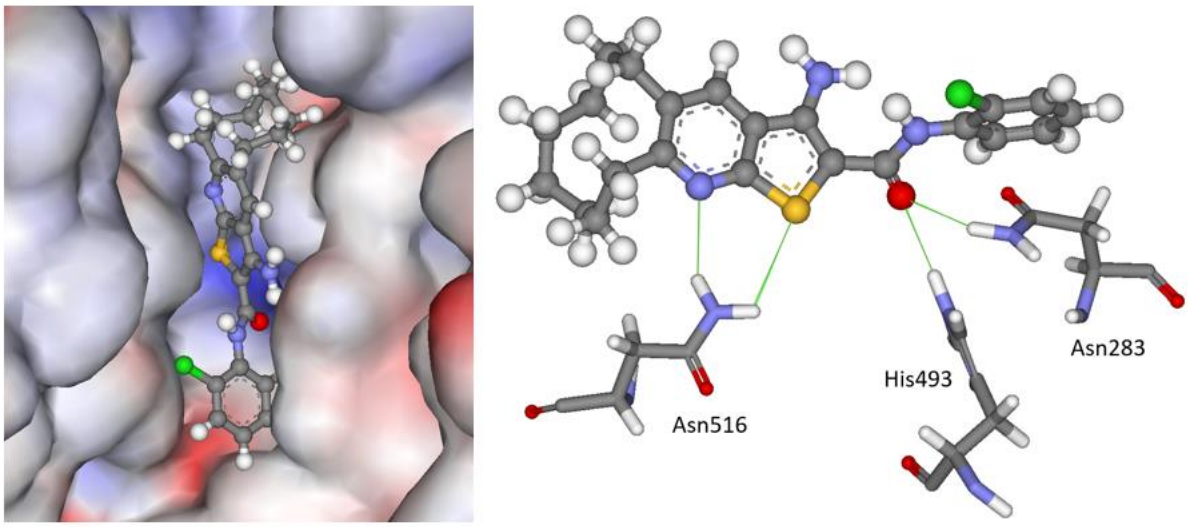

A **B**

Figure S8: The docked configuration of DJ282 in the binding site of TDP1 as predicted using the GoldScore scoring function. (A) The protein surface is rendered. The ligand occupies the binding pocket blocking access to it. Blue depicts a hydrophilic region with a partial positive charge on the surface; red depicts regions with a partial negative charge and grey shows neutral areas. (B) H-bonds are shown as green lines between DJ282 and the amino acids His493 and Asn516 side groups.

Figure S9: Comparison of our solved TDP1$_{149\text{-}608}$ structure (green) with the published TDP1$_{149\text{-}608}$ structure (hot pink, PDB ID: 1JY1).[2]

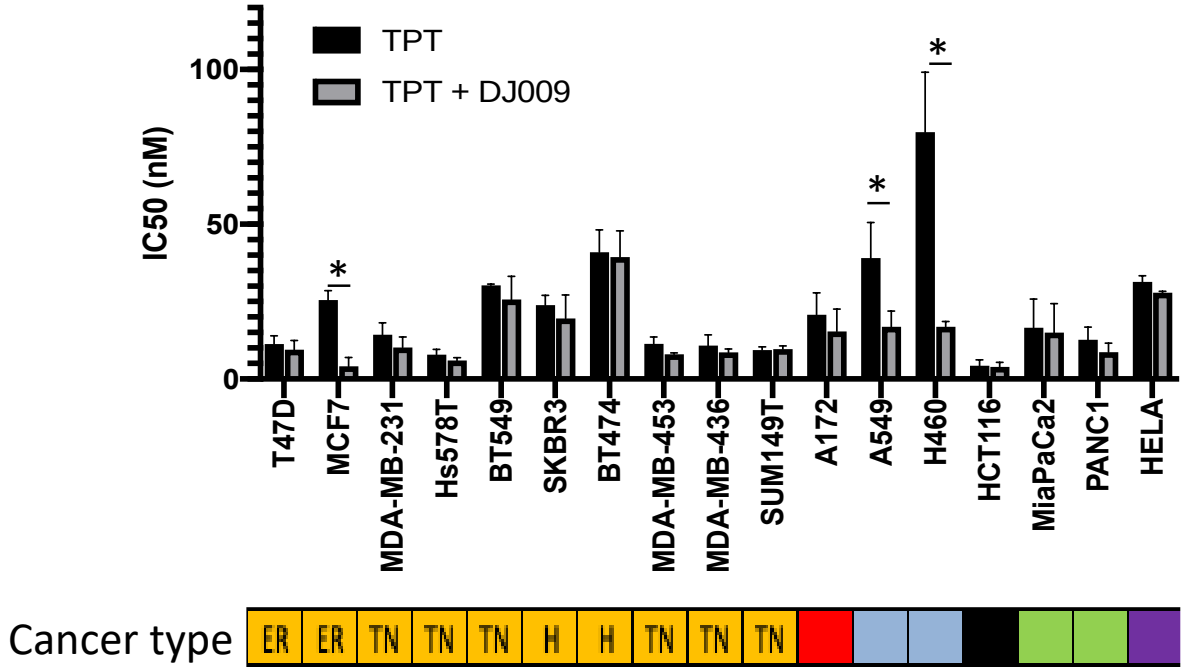

Figure S10: The half maximal inhibitory concentration (IC50) for a panel of cancer cell lines treated with a combination of topotecan (TPT) and DJ009. Significant difference * $p < 0.05$. Data are mean ± SE of three independent experiments.

ER – Estrogen Responsive, H-Her2 positive, TN- Triple Negative. Cancer types: orange – breast cancer, red - glioblastoma, blue – lung cancer, black – colon carcinoma, green – pancreatic and violet – cervical. The lung cancer cell line H460 demonstrates a pronounced effect when treated with a combination of both TPT and DJ009.

(a)

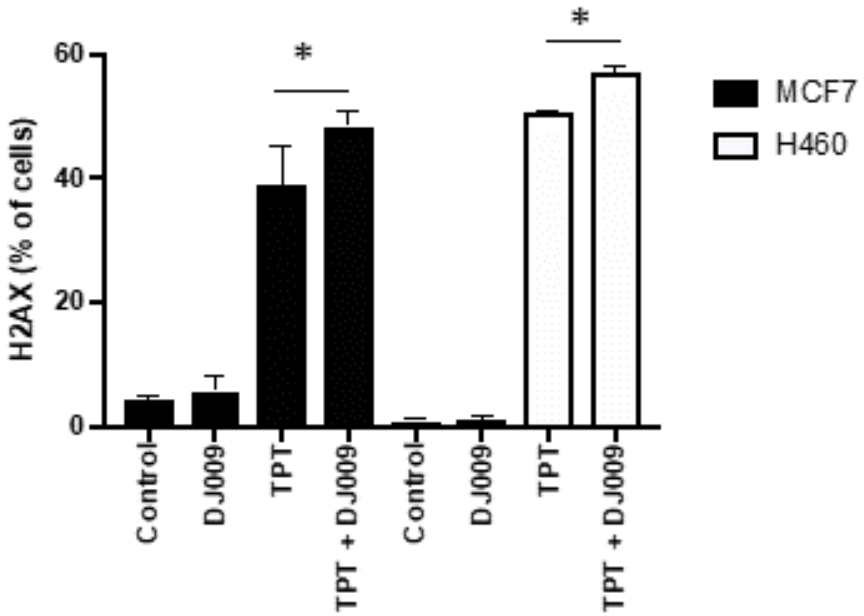
H2AX (% of cells)
60
40
20
0
*
*
MCF7
H460
Control
DJ009
TPT
TPT + DJ009
Control
DJ009
TPT
TPT + DJ009

(b)

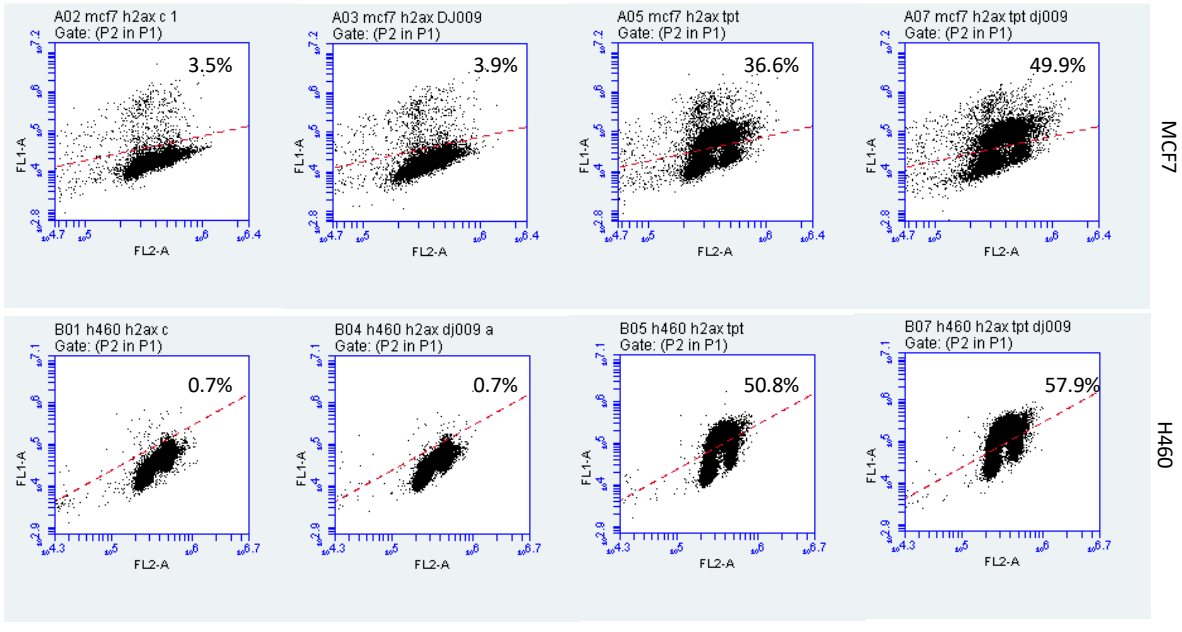
A02 mcf7 h2ax c 1
Gate: (P2 in P1)
3.5%
A03 mcf7 h2ax DJ009
Gate: (P2 in P1)
3.9%
A05 mcf7 h2ax tpt
Gate: (P2 in P1)
36.6%
A07 mcf7 h2ax tpt dj009
Gate: (P2 in P1)
49.9%
B01 h460 h2ax c
Gate: (P2 in P1)
0.7%
B04 h460 h2ax dj009 a
Gate: (P2 in P1)
0.7%
B05 h460 h2ax tpt
Gate: (P2 in P1)
50.8%
B07 h460 h2ax tpt dj009
Gate: (P2 in P1)
57.9%
FL1-A
FL2-A
MCF7
H460
Control
DJ009
TPT
DJ009 + TPT

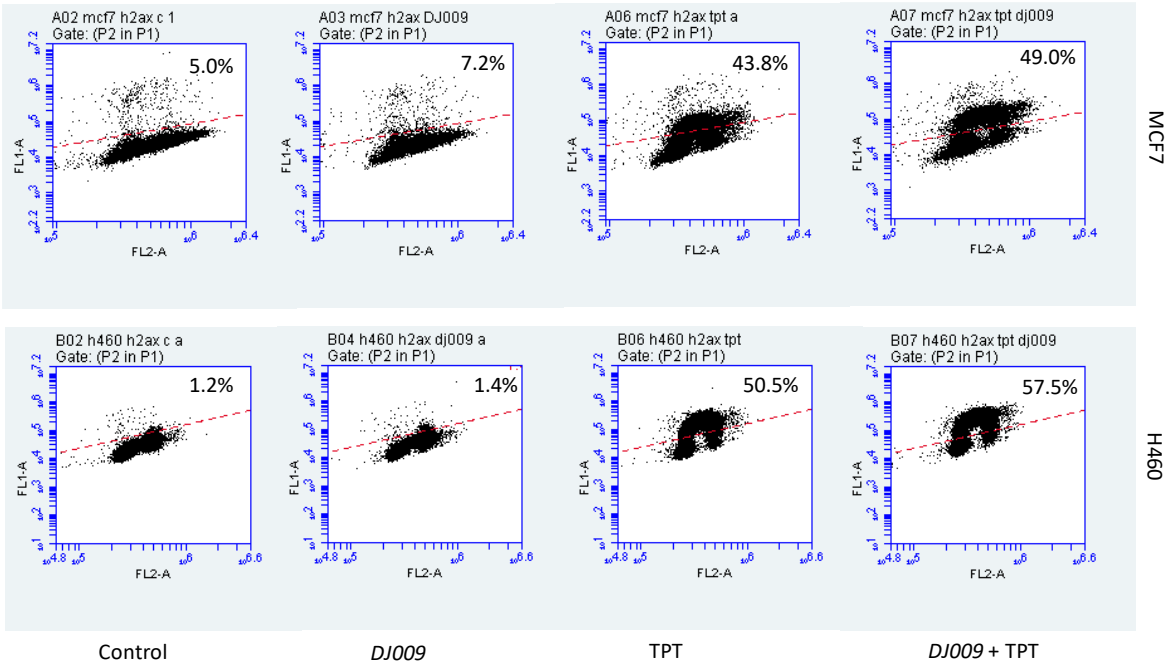

Figure S11: (a) The results of the γ-H2AX assay indicating the amount of DNA double strand breaks in the cancer cell lines MCF7 and H460. Administration of DJ009 had significant enhancement of the effect of topotecan (TPT). Data are mean ± SE of three independent experiments; (b) Comparison of flow cytometry profiles following treatment for 2 h showed a S-phase specific DNA damage profile with significant γ-H2AX increase in treatment combination of DJ009 and topotecan than only topotecan.

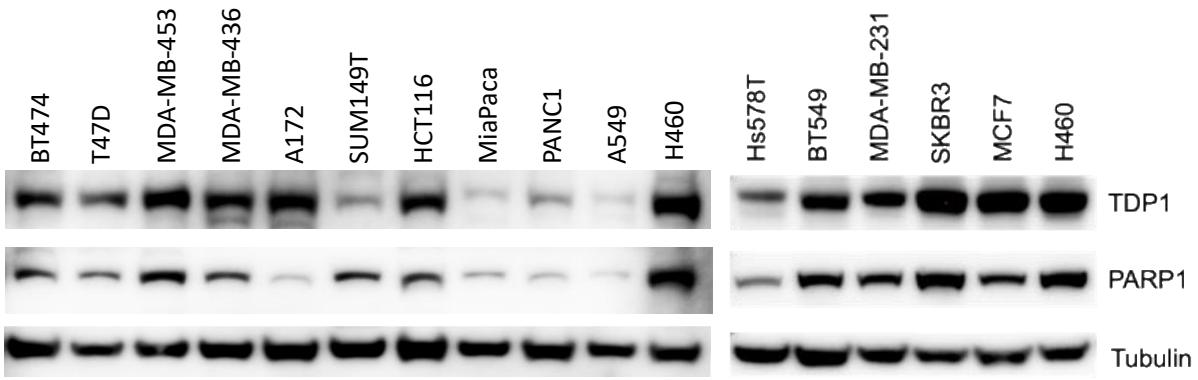

Figure S12: Immunoblotting analysis showing relative expression of TDP1 as well as PARP1 (Poly(ADP-ribose) polymerase-1) in a panel of cancer cell lines. Tubulin was used as a reference.

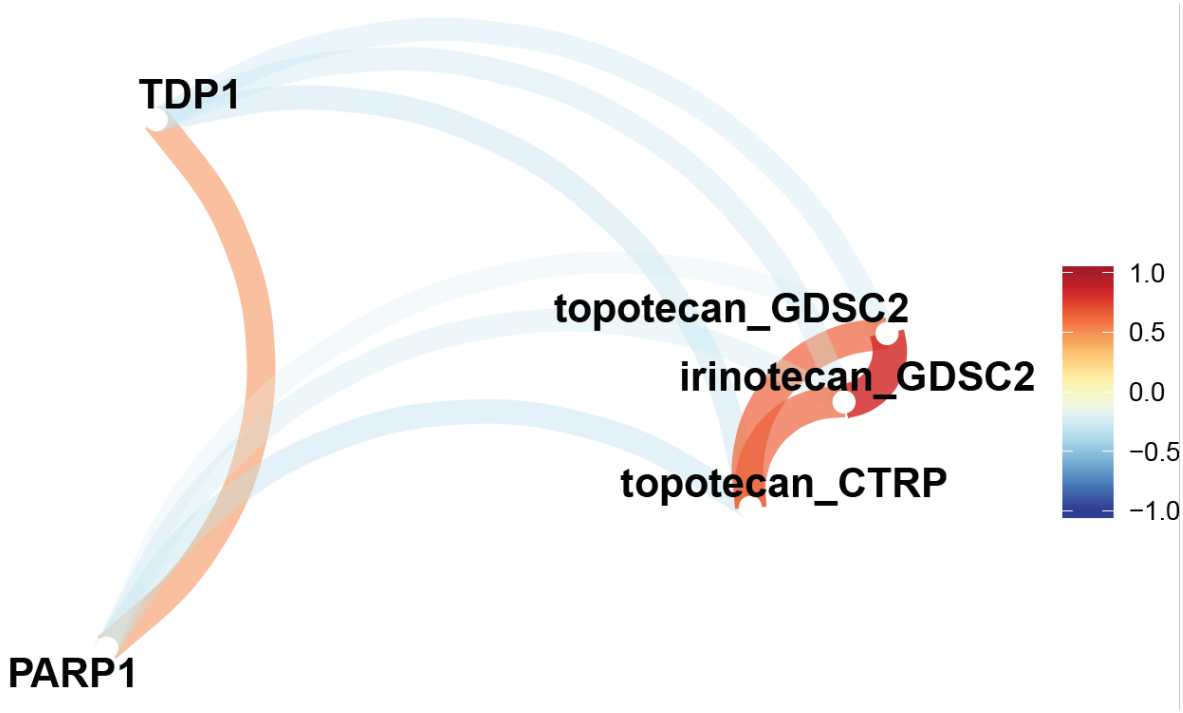

Figure S13: TOP1 poisons irinotecan/topotecan (TPT) and their TDP1 and PARP1 expression in 358 cancer cell lines. The closer the nodes, the more correlated they are. Shorter, wider and more opaque paths represent stronger correlations between the nodes and vice versa. Red and blue colours indicate positive and negative Spearman's correlations, respectively. Paths connecting nodes correlating < |0.25| were omitted. The network correlation plots were rendered using corrr package in R.[3]

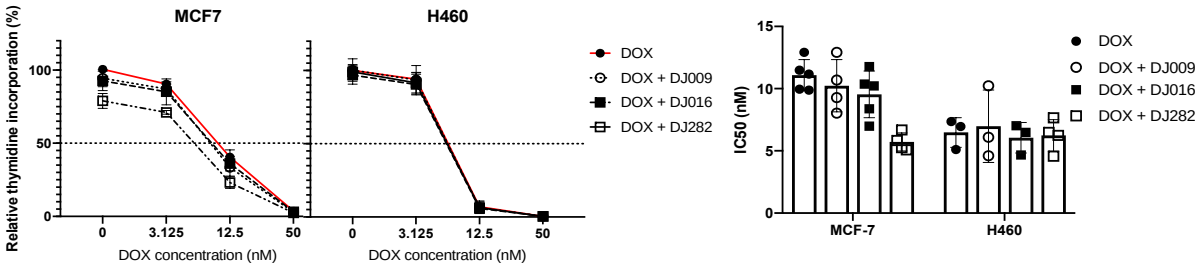

Figure S14: The dose response plots and corresponding bar graphs with the IC_{50} values of the different potency of each TDP1 inhibitors in combination with doxorubicin (DOX) in MCF7 breast cancer and H460 lung cancer cell line. The concentration of each TPs was 430 nM for all the experiments.

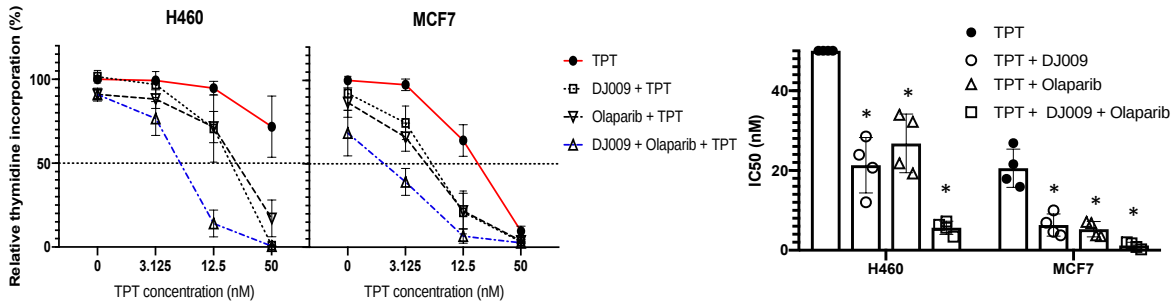

Figure S15: The dose response plots and corresponding bar graphs with the IC_{50} values of the different potency of each TDP1 inhibitors in combination with TPT and the PARP1 drug olaparib in MCF7 breast cancer and H460 lung cancer cell line. The concentration of each TPs was 430 nM for all the experiments. Significant differences were observed between TPT alone versus TPT in combination with DJ009, olaparib or DJ009 plus olaparib. * $p<0.05$ and data are mean ± SE of three independent experiments.

Supplementary Tables

Table S1: Data collection and refinement statistics for human $TDP1_{149-608}$ X-ray crystallography

	Human $TDP1_{149-608}$
Data Collection	
Diffraction source	MX2, Australian Synchrotron
Wavelength (Å)	0.9537
Temperature (K)	100
Detector	Eiger X 16M
Rotation (°)	360
Collection time (s)	36
Space group	$P2_12_12_1$
a,b,c (Å)	50.24,105.13,194.28
α,β,γ, (°)	90.00,90.00,90.00
Mosaicity	0.06
Resolution range (Å)*	48.64-2.13 Å (2.19-2.13)
No. of unique reflections*	58349 (437)
Completeness (%)*	99.7 (96.7)
Multiplicity (%)*	13.7 (12.8)
Rpim*	0.04 (0.21)
<I/σ(I)>*	11.3 (2.7)
$CC_{1/2}$*	0.998 (0.888)
Refinement	
Resolution range (Å)	48.69-2.13

No. reflections, working	52486
No. reflections, test	2894
R_{cryst}	0.187
R_{free}	0.224
Number of atoms	
Protein	6812
Solvent	281
Av. B factors (Å^2)	
Protein	30.8
Solvent	32.6
R.m.s deviation	
Bond lengths	0.006
Bond angles	1.36
Ramamchandran favoured (%)	97.5
Molprobity score (percentile)	99th percentile

*Numbers in brackets are for the outer shall data (2.19-2.13 Å)

Table S2: The binding scores for the scoring functions used.

Ligand	ASP	ChemScore	GoldScore	ChemPLP	TDP1 inhibition
DJ009	28.5	28.7	47.6	53.1	36%
DJ016	29.6	27.6	51.0	51.5	32%
DJ282	31.2	32.2	52.0	60.3	0.5 µM

Supplementary References

1. Zakharenko, A. L.; Luzina, O. A.; Sokolov, D. N.; Kaledin, V. I.; Nikolin, V. P.; Popova, N. A.; Patel, J.; Zakharova, O. D.; Chepanova, A. A.; Zafar, A.; Reynisson, J.; Leung, E.; Leung, I. K. H.; Volcho, K. P.; Salakhutdinov, N. F.; Lavrik, O. I. Novel tyrosyl-DNA phosphodiesterase 1 inhibitors enhance the thera-peutic impact of topotecan on in vivo tumor models. Eur. J. Med. Chem. 2019, 161, 581–593.
2. Davies, D. R.; Interthal, H.; Champoux, J. J.; Hol, W. G. J. The crystal structure of human tyrosyl-DNA phosphodiesterase, Tdp1. Structure 2002, 10, 237-248.
3. Jackson, S. corrr: Correlations in R. R package version 02.1. 2016. https://cran.r-project.org/web/packages/corrr/index.html. Accessed 4 June 2018.